Size, albedo, and rotational period of the Hayabusa2# target (98943) 2001 CC21

S. Fornasier, E. Dotto, P. Panuzzo, M. Delbo, I. Belskaya, Y. Krugly, R. Inasaridze, M. A. Barucci, D. Perna, J. Brucato, et al.

A&A, 688, L7 (2024)
https://doi.org/10.1051/0004-6361/202450447

Astronomy & Astrophysics

LETTER TO THE EDITOR

Size, albedo, and rotational period of the Hayabusa2# target (98943) 2001 CC21

S. Fornasier[1,2], E. Dotto[3], P. Panuzzo[4], M. Delbo[5,6], I. Belskaya[7,1], Y. Krugly[7], R. Inasaridze[8,9], M. A. Barucci[1], D. Perna[3], J. Brucato[10], and M. Birlan[11,12]

[1] LESIA, Université Paris Cité, Observatoire de Paris, Université PSL, CNRS, Sorbonne Université, 5 place Jules Janssen, 92195 Meudon, France
e-mail: sonia.fornasier@obspm.fr
[2] Institut Universitaire de France (IUF), 1 rue Descartes 75231 Paris Cedex 05, France
[3] INAF-Osservatorio Astronomico di Roma, 00078Monte Porzio Catone (Roma), Via Frascati 33, Italy
[4] GEPI, Observatoire de Paris, Université PSL, CNRS, Place Jules Janssen, 92195 Meudon, France
[5] Université Côte d'Azur, CNRS-Lagrange, Observatoire de la Côte d'Azur, CS 34229, 06304 Nice Cedex 4, France
[6] School of Physics and Astronomy, University of Leicester, Leicester, UK
[7] Institute of Astronomy, V.N. Karazin Kharkiv National University, 4 Svobody Sq., Kharkiv 61022, Ukraine
[8] E. Kharadze Georgian National Astrophysical Observatory, Abastumani, Georgia
[9] Samtskhe-Javakheti State University, Akhaltsikhe, Georgia
[10] INAF-Astrophysical Observatory of Arcetri, Largo E. Fermi 5, 50125 Firenze, Italy
[11] IMCCE, Observatoire de Paris, CNRS, PSL Research University, 77 av. Denfert Rochereau, 75014 Paris Cedex, France
[12] Astronomical Institute of the Romanian Academy, 5 Cutitul de Argint, 040557, sector 4, Bucharest, Romania

Received 19 April 2024 / Accepted 17 July 2024

ABSTRACT

Aims. This study aims to determine the size, albedo, and rotational period of (98943) 2001 CC21, a target of the Hayabusa2 extended mission, using thermal data from the *Spitzer* Space telescope and ground-based observations.
Methods. The *Spitzer* data were acquired with the Infrared Spectrograph in the 6–38 μm range, reduced using the *Spitzer* pipeline, and modeled with the near-Earth asteroid thermal model to determine the asteroid size and albedo. The absolute magnitude and rotational period were determined thanks to new observations carried out at the 3.5 m New Technology Telescope, the 1.2 m Observatoire de Haute Provence, and the 0.7 m Abastumani telescope. Three complete light curves were obtained in 2023 and 2024 at the last-mentioned telescope.
Results. We determine an absolute magnitude of $H = 18.94 \pm 0.05$ and a rotational period of 5.02124±0.00001 hours, with a large light curve amplitude of ~0.8 mag. at a phase angle of 22°, indicating a very elongated shape with an estimated a/b semiaxis ratio ≥1.7, or a close-contact binary body. The emissivity of 2001 CC21 is consistent with that of silicates, and its albedo is 21.6±1.6%. Finally, the spherical-equivalent diameter of 2001 CC21 is 465±15 m.
Conclusions. The albedo value and emissivity determined here, coupled with results from polarimetry and spectroscopy from the literature, confirm that 2001 CC21 is an S-complex asteroid, and not an L-type one as was previously suggested. The size of 2001 CC21 is less than 500 m, which is smaller than its first size estimation (~700 m). These results are relevant in preparation of the observing strategy for 2001 CC21 of the Hayabusa2 extended mission.

Key words. methods: data analysis – methods: observational – techniques: photometric – minor planets, asteroids: individual: (98943) 2001 CC21

1. Introduction

The Japan Aerospace Exploration Agency's (JAXA) Hayabusa2 mission, following the successful return of the Ryugu samples in December 2020, has been extended to explore two more near-Earth asteroids (NEAs): (98943) 2001 CC21, which is scheduled for a flyby in 2026, and the fast-spinning 1998 KY26, due for a rendezvous in 2031. The extended mission has been nicknamed Hayabusa2#, where the # character stands for "SHARP" (small hazardous asteroid reconnaissance probe). Several observing campaigns of these two targets have been and will be carried out to better understand their physical properties in support of the Hayabusa2# mission, and in particular to optimize the observing strategy.

This paper focuses on 2001 CC21, which is an Apollo NEA. The first spectrum of NEA (98943) 2001 CC21 was obtained during the MITNEOS survey in October 2004 and led to an L-type taxonomic classification (Binzel et al. 2004, 2019). This type of asteroid should be rich in calcium-aluminum inclusions (Sunshine et al. 2008) and have a flat spectrum in the 0.75–1 μm region. However, other spectra obtained in the literature (Lazzarin et al. 2005; Geem et al. 2023) clearly indicate the presence of well-defined absorption features in the 0.9–1 μm range and around 2 μm, associated with the presence of

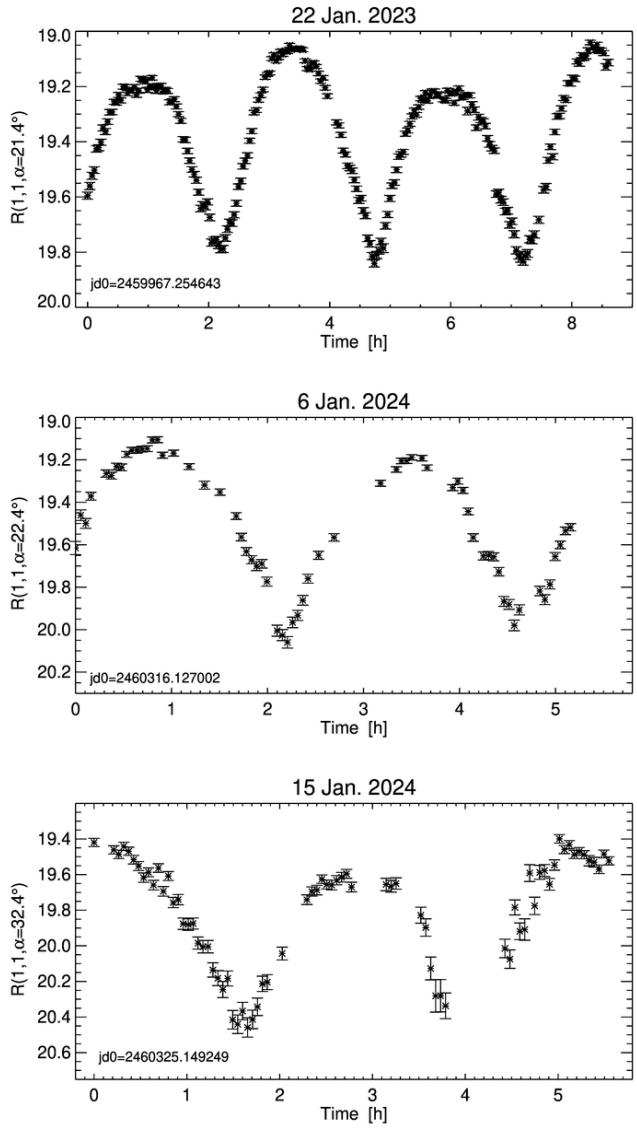

Fig. 1. (98943) 2001 CC21 light curves, in reduced R magnitude, acquired on January 22, 2023 and on January 6 and 15, 2024 at the 0.7 m Abastumani telescope.

pyroxene. Therefore, 2001 CC21 belongs to the S-complex and has been classified as Sq, Sk, or Q type in the Bus-Demeo classification scheme (DeMeo et al. 2009).

In addition, the polarimetric properties of 2001 CC21 determined by Geem et al. (2023) are consistent with those of S-complex asteroids and different from those of L-type ones. These authors also obtained the first measurements of the target albedo of 23±4% from the polarimetric slope, and estimated a size ranging from 440 m to 530 m.

This body is known to have an elongated shape, with a light curve amplitude of 0.75–1.1 in magnitude, and a rotational period of 5.0159 h (Warner 2023), or 5.0247 h[1].

In this paper, we present the results of the analysis of the spectral energy distribution (SED) of 2001 CC21 obtained by the *Spitzer* Space Telescope in the 6–38 μm range, which allows us to accurately estimate the size and albedo of the target. We also present ground-based observations in photometry performed to determine the rotational period of 2001 CC21 and its absolute magnitude. The latter is a basic input parameter of the thermal model.

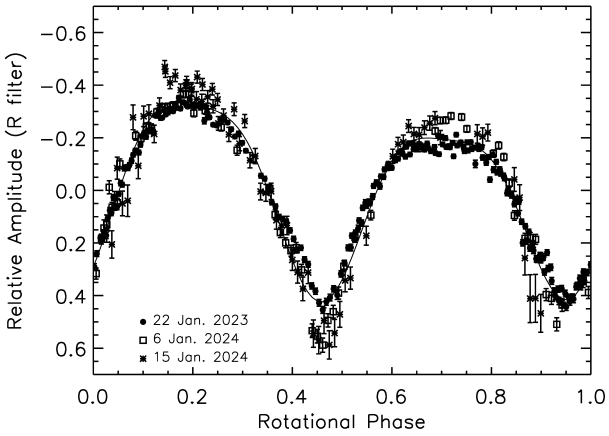

Fig. 2. Composite light curve of 2001 CC21. The zero phase time corresponds to JD 2460100.

2. Rotational period and photometry

To support the *Spitzer* data interpretation, we carried out photometry of 2001 CC21 on October 31, 2005 at the 3.58 m New Technology Telescope (NTT). We used the EMMI instrument in the V, R, and I filters centered at 543, 641, and 799 nm, coupled with a 2048×4096 CCD that has squared pixels of 15 μm. Further photometric observations were conducted at the 1.2 m telescope of the Observatoire de Haute Provence (OHP) in November 2022 in the broadband Johnson B, V, R, and Gunn I filters. The data were collected with a 2048×2048 detector in 2×2 binning mode, resulting in a pixel scale of 0.77 arcsec px^{-1}.

Additionally, three light curves were obtained in the Johnson-Cousins R filter at 0.7 m Abastumani Miniscus telescope (Georgia) in January 2023 and 2024 (Fig. 1). These observations were obtained with a 2048×2048 CCD in unbinning mode with a pixel scale of 1.3 arcsec px^{-1}. The data were reduced in the standard way (Fornasier et al. 2004). Fluxes were extracted via aperture photometry and absolutely calibrated using different standard stars observed during each night (Landolt 1992). The observing conditions and results are reported in Table A.1. The uncertainties in magnitude and colors take into account both instrumental and calibration errors.

We applied the standard Fourier analysis (Harris 1989) to these light curves, obtaining a rotation period of 5.02124±0.00001 hours. This value is also confirmed when we include in our analysis two light curves obtained on January 31 and February 1, 2023 with the 0.3 m telescope (Observatorio Estelia Ladines, Asturias, Spain) and publicly available in the Asteroid Lightcurve Data Exchange Format (ALCDEF) database[2]. Fig. 2 shows the composite light curve obtained by combining the three single-night light curves reported in Fig. 1.

The amplitude of the light curve changed from 0.77 in 2023 to 0.86 in 2024 at a phase angle of about 22°, and increased to 1 mag for observations at a phase angle of 33°. In the literature, the highest amplitude of 1.1 mag was measured by Pravec in 2022 at a phase angle of 68°. Considering the light curve amplitudes measured in 2002–2024 in the literature and in this paper, and the amplitude-phase angle relationship for S-type asteroids (Zappala et al. 1990), the 2001 CC21 amplitude reduced to a

[1] https://www.asu.cas.cz/~ppravec/newres.txt

[2] https://alcdef.org/

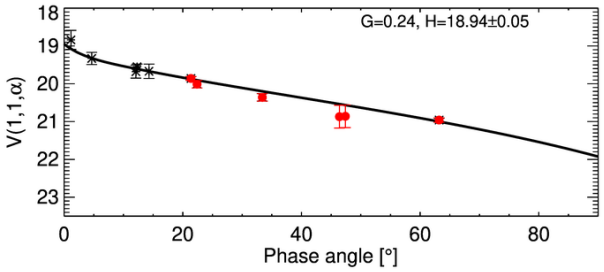

Fig. 3. HG fit of the photometric data presented here (Table A.1, red circles), together with data from astrometry available in the MPC database.

zero phase angle is in the range of 0.36–0.58 mag. Using the largest reduced amplitude, we estimate for 2001 CC21 an elongated shape with an a/b half-axis ratio ≥1.7. Since the light curves show broad maxima and sharp minima, we can assume a contact binary nature for this asteroid, although it is impossible to distinguish an elongated object from a contact binary one based on the light curve shape alone (Harris & Warner 2020).

To compute the absolute magnitude, we used the entire dataset presented in this paper, as well as data available in the literature. Numerous estimations of the asteroid's magnitudes were made during its astrometric observations in 2001–2024 covering the wide phase angle range from 1 to 96°. These data are available in the MPC database[3]. To obtain the phase curve, we used magnitude measurements in the V and R bands, and we assumed a $V - R$ color index of 0.43, which is the average value determined from NTT and OHP observations (Table A.1), to combine all of the measurements in the V band. We calculated the average magnitude from astrometric observations at a given phase angle using typically five to ten measurements, and we took the standard deviation as the magnitude error.

We first applied the HG system (Harris 1989), assuming a G value of 0.24, which is the standard value for S-type asteroids (Warner et al. 2009; Pravec et al. 2012), including the data presented in Table A.1 and some data from the literature covering the smaller phase angle values. The mean magnitudes from the light curve studies and the NTT observations taken a few weeks before the *Spitzer* one (which turned out to be taken close to the light curve mean, as is shown in Sect. 3) were given a higher weight in the fit. The derived H value (in the V filter) is $H = 18.94 \pm 0.05$ (Fig. 3).

We also checked the consistency of this result by analyzing all the data presented here and those available from the literature with the HG1G2 system (Muinonen et al. 2010). We obtained $H = 18.92 \pm 0.20$, $G1 = 0.2588$, and $G2 = 0.3721$ (Fig. A.1). The large uncertainty in the absolute magnitude is due to the wide amplitude of the 2001 CC21 light curve, and the large error bars of the astrometric observations.

3. *Spitzer* observations and data reduction

NEA (98943) 2001 CC21 was observed on November 20, 2005 from 10:17 to 12:26 UT with the Infrared Spectrograph (IRS, Werner et al. 2004) on board the *Spitzer* Space Telescope. Data were acquired in the low-resolution mode ($R = \lambda/\Delta\lambda \sim 64$–128) covering the 5.2–38 μm range using the four IRS long slit segments: the first and second orders of the short wavelength, covering the 7.4–14.2 μm (SL1) and 5.2–8.5 μm (SL2) wavelength ranges, respectively; and the first and second orders of the long wavelength segment, covering the 19.5–38.0 μm (LL1) and the 14.0–21.5 μm ranges (LL2), respectively. The individual ramp times and the total exposure time are reported in Table 1 together with the observing conditions of 2001 CC21.

Table 1. Observational details of 2001 CC21 with *Spitzer*/IRS (Seg. represents the segment's name).

Date	UT_{start}	T_{ramp} (s)	Total T_{exp} (s)	Seg.
2005-11-20	10:17:06.340	14.68	88.08	SL2
2005-11-20	10:19:37.039	14.68	88.08	SL2
2005-11-20	10:22:10.339	14.68	58.72	SL1
2005-11-20	10:23:57.042	14.68	58.72	SL1
2005-11-20	10:26:10.245	121.9	1218.96	LL2
2005-11-20	10:51:21.747	121.9	1218.96	LL2
2005-11-20	11:16:33.242	121.9	2437.92	LL1
2005-11-20	12:06:47.737	121.9	2437.92	LL1

Notes. The observations were carried out at heliocentric and target-*Spitzer* distances of 1.16824 au and 0.29372 au, respectively, and at a phase angle of 52.6°.

The data were reduced starting from the basic calibrated data generated by the *Spitzer* Space Center automated pipeline, which are corrected for flat fielding, dark current, stray light, and cosmic rays, and absolutely calibrated in flux (Houck et al. 2004). The sky background was removed by differencing two consecutive images taken at different nodding positions for each spectral segment.

Finally, we used the *Spitzer* IRS Custom Extraction (SPICE) software to extract the one-dimensional spectra for each of the four IRS segments (Houck et al. 2004), following the methodology and the steps described in Lamy et al. (2008), and Barucci et al. (2008).

The estimated photometric uncertainties are typically ±2%, but can reach 5% at the edges of the different segments[4].

For each IRS segment, we have two nodding positions, so two independent spectra to average. The observations of 2001 CC21 cover about half of the rotation period, and therefore span the full light curve amplitude. In particular, flux differences between the first (named a) and the second (named b) nodding positions of the LL1 and LL2 segments (Fig. A.2) are clearly visible, while there are no flux variations for the a and b positions of the SL1 and SL2 segments due to the relatively short exposure time.

Special care was therefore taken in combining the four segments according to the light curve: the LL2a and LL1a spectra are at a similar flux level, while the LL2b and LL1b spectra have a lower and higher flux corresponding to the maximum and minimum of the visible light curve, respectively. We present in Fig. 4 the January 2023 light curve with the estimated positions of the four IRS segment observations superposed, in color. These positions were estimated considering both the time interval between each *Spitzer* spectrum and the SL2a start time, and the differences between the thermal fluxes of two adjacent spectra, converted in ΔH_v. To combine the SED of the four segments, we proceeded as follows: a) we used the mean spectra for each of the four segments; b) the SL1 and SL2 segments were naturally connected, because the flux was at the same level; c) we shifted the LL2 mean spectrum to match the latest wavelengths of the

[3] https://www.minorplanetcenter.net/db_search/show_object?object_id=98943

[4] https://irsa.ipac.caltech.edu/data/SPITZER/docs/irs/irsinstrumenthandbook/IRS_Instrument_Handbook.pdf

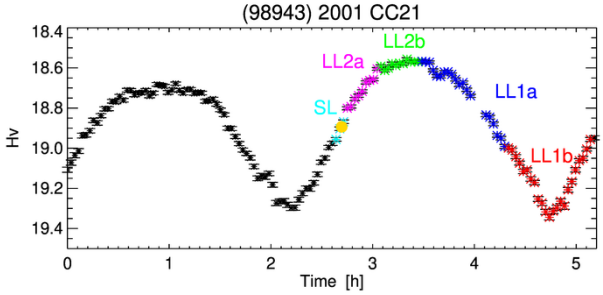

Fig. 4. Light curve of 2001 CC21, in absolute magnitude, obtained on January 22, 2023 with the 0.7 m Abastumani telescope. The approximate estimated positions of the *Spitzer* observations are shown in color. The yellow circle represents the H_v magnitude derived from the NTT telescope observations acquired three weeks prior to the *Spitzer* ones.

SL1 one; and d) we shifted the LL1 mean spectrum to properly connect it to the shifted LL2 mean spectrum.

Given the previously determined rotation period, the NTT observations, taken 3 weeks before the *Spitzer* data, fall at a rotational phase of +0.0149 after the start of the *Spitzer* data, corresponding to a difference of 4.52 minutes. The absolute magnitude of the NTT observation (yellow symbol in Fig. 4) is 18.89±0.05, assuming $G = 0.24$.

Considering that we had merged the *Spitzer* data with respect to the SL segments, and that the ~ 2.5 h duration of the observations covers the full amplitude of the light curve, we decided to take as the absolute magnitude value for the thermal modeling the one corresponding to the mean value of the light curve obtained with the HG system; that is, 18.94±0.05. This value is also very close to the one determined from the NTT observations.

4. Size, albedo, and emissivity

To determine the size (diameter, D) and albedo (p_v) of 2001 CC21, we used the near-Earth thermal model (NEATM, Harris 1998, for details see Appendix B).

Using $H_v = 18.94\pm0.05$, the NEATM best-fit results for the 2001 CC21 SED are as follows: a diameter of 465±15 m, an albedo of $p_V = 21.6\pm1.6\%$, and a beaming parameter of $\eta = 1.847\pm0.034$. The uncertainties take into account the flux errors, and the *Spitzer* uncertainties in the absolute flux values (we used a conservative value of 5%)[5]. The derived subsolar temperature (T_{SS}) is 312 K. The observed SED and the NEATM model that best fits the data are shown in Fig. 5. The derived diameter is much lower than the 700 m originally evaluated (Hirabayashi et al. 2021), and it falls in the size estimate (440–530 m) from polarimetric observations (Geem et al. 2023). These authors also found an albedo value of 23±4%, very close to the one determined here. Additional thermal data were obtained by NEOWISE and led to a preliminary 2001 CC21 size assessment of 329^{+78}_{-41} m, a value smaller than the one we found, and with much larger uncertainties (Wright et al. 2023). Finally, on March 5, 2023, a stellar occultation of 2001 CC21 was observed[6], giving an occultation chord of 449±12 m. Therefore, the minimal projected dimension of this NEA should be 449 m. With the rotational period estimated here, this event falls at 1.46 h after the zero reference time in the light curve taken on January 23, 2023 (Fig. 1). The corresponding magnitude is in between the secondary maximum and the light curve mean, so the projection of this chord should roughly correspond to the equivalent spherical shape diameter of 2001 CC21.

The η value of 2001 CC21 is relatively high compared to the 0.756 value used in the standard thermal model of main belt asteroids (Lebofsky et al. 1986), but rather common for NEAs observed at a relatively high phase angle (Mainzer et al. 2014). Indeed, the *Spitzer* observations were made at a phase angle of 52.6°, and a correlation between η and α has been reported in the literature (Delbo 2004; Wolters et al. 2008; Mainzer et al. 2011, 2014). In fact, in the NEATM model, the beaming parameter increases at higher phase angles to compensate for the loss of the thermal flux, which is normally sent mostly in the sunward direction. Wolters et al. (2008) reported a possible anticorrelation between η and p_v (their Fig. 9g) for S- and Q-type NEAs. The η and p_v values we found for 2001 CC21 fit very well with the line showing the anticorrelation mentioned above (Wolters et al. 2008). The 2001 CC21 albedo and beaming parameter values are close, within uncertainties, to those found for the binary NEAs (5381) Sekhmet and 2003 YT1 (Delbo et al. 2011), even though these bodies are at least three times larger than the Hayabusa2# target and rotate faster (rotation period of 2.3–2.5 h). Considering also the shape of the visible light curve, this may support the hypothesis that 2001 CC21 is a contact binary, even though this cannot be conclusively deduced by the thermal properties. More generally, Apollo NEAs have η values peaking at about 1.3, but with a large distribution including values in the 0.8–3 range (Mainzer et al. 2012). These last authors reported larger η values for the Aten population than for the Apollo one, but stress that this difference may simply be correlated with the larger phase angle conditions of Aten versus Apollo observations.

As the shape and spin state of 2001 CC21 remain undetermined, thermophysical models (TPMs) cannot be readily employed. The principal advantage of utilizing a TPM for the analysis of thermal IR data is its capability to ascertain the surface thermal inertia, which is a parameter that quantifies the resistance to temperature changes. Thermal inertia can be used to constrain the nature of the surface (see Delbo et al. 2015, for a review). Nevertheless, thermal inertia can still be estimated from the beaming parameter value and knowledge of the rotation period and albedo of an asteroid using the method proposed by Harris & Drube (2016), although with less accuracy compared to using the TPM. The application of this method to 2001 CC21 data results in a thermal inertia of 398±8 J m^{-2} s$^{-0.5}$ K^{-1}, using Eq. (2) from Harris & Drube (2016), and assuming the asteroid to have a 90° aspect angle, which is the most likely solution (Fatka et al. 2023). In fact, it has been observed that most small NEAs are in Yarkovsky-O'Keefe-Radzievskii-Paddack end states with an obliquity of 90 degrees. However, the thermal inertia estimated by this method is a function of the unknown aspect angle of 2001 CC21: the lower the aspect angle, the higher the estimated thermal inertia value would be according to the curve shown in Fig. B.1. Therefore, we determine here a lower limit of the thermal inertia for 2001 CC21, which should be strictly taken as the nominal value minus 3 σ of the aforementioned uncertainty. This corresponds to a lower limit of ~370 J m^{-2} s$^{-0.5}$ K^{-1}. However, we stress that this value is a preliminary estimation derived from the η value and using the NEATM model, which assumes a spherical shape that is obviously not the one of 2001 CC21. A thermal inertia >370 J m^{-2} s$^{-0.5}$ K^{-1} is typical of NEAs the size of 2001 CC21 (see Fig. 7 in Novaković et al. 2024). Based on the assumption of

[5] https://irsa.ipac.caltech.edu/data/SPITZER/docs/irs/irsinstrumenthandbook/IRS_Instrument_Handbook.pdf
[6] http://www.unmannedspaceflight.com/index.php?showtopic=4920&pid=262173&st=975&#entry262173

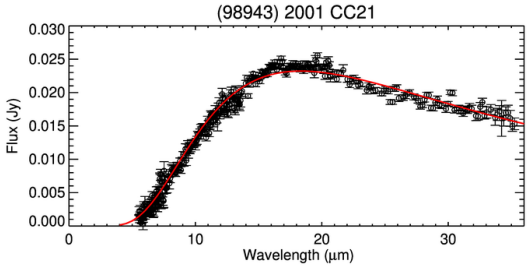

Fig. 5. Spectral energy distribution of (98943) 2001 CC21 with the best NEATM fit (red line) superposed.

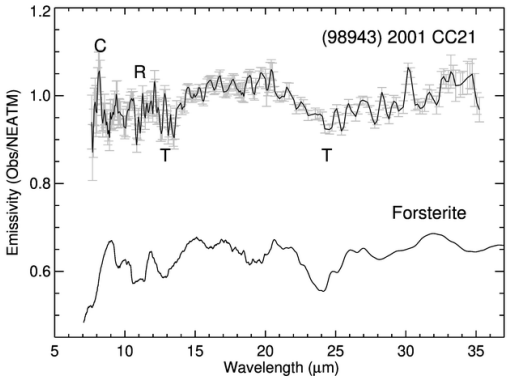

Fig. 6. Spectral emissivity of (98943) 2001 CC21, with the associated uncertainties (gray symbols), compared with the laboratory emissivity of forsterite. Christiansen, Reststrahlen, and transparency features are noted as C, R, and T, respectively.

an ordinary chondrite composition and thermal properties, it can be reasonably inferred that the lower limit of the thermal inertia estimated here is related to a surface comprising a mixture of regolith and exposed rocks.

Figure 6 shows the emissivity that we obtained for 2001 CC21, as the ratio of the *Spitzer* spectrum to the NEATM best-fit model (Fig. 5). The main features observable in this range are the Christiansen peak, Reststrahlen, and transparency features. The Christiansen peak is associated with the principal molecular vibration band and for silicates occurs between 7.5 and 9.5 μm. In the 2001 CC21 emissivity spectrum, it appears at about 8 μm. The Reststrahlen features, due to the vibrational modes of molecular complexes, have a lower contrast for smaller grain sizes and appear as a plateau between 9 and 12 μm. Transparency features occur in the spectral region in which the absorption coefficient decreases and grains become more transparent. For 2001 CC21, they occur at about 12 μm, with a secondary feature at ~24 μm. In order to interpret these features above the thermal continuum in terms of the surface composition of 2001 CC21, we compared its emissivity with that of minerals and meteorites acquired by our group and published by Dotto et al. (2004, 2000) and Barucci et al. (2002), or available in the literature (Salisbury et al. (1991a,b), the ASTER spectral library[7], and the RELAB database[8]). On the basis of this analysis, the emissivity spectrum of our target seems to be in good agreement with the laboratory emissivity spectrum of forsterite, a Mg_2SiO_4 silicate of the olivine group. 2001 CC21 also confirms its silicatic nature in this wavelength range.

[7] http://speclib.jpl.nasa.gov
[8] https://sites.brown.edu/relab/relab-spectral-database

5. Conclusion

Utilizing thermal data from the *Spitzer* Space Telescope and novel ground-based observations, we have derived the most precise estimation to date of the diameter (465±15 m), albedo (21.6±1.6%), and rotational period (5.02124±0.00001 hours) of (98943) 2001 CC21. Its thermal inertia, estimated from the beaming parameter, is $>370\,J\,m^{-2}\,s^{-0.5}\,K^{-1}$. The albedo and emissivity determined here, along with results derived from polarimetry and spectroscopy in the literature, confirm that the Hayabusa2# extended mission target is an S-complex asteroid. The results presented here indicate that 2001 CC21 is either an elongated asteroid with an a/b ratio of ≥1.7, or a contact binary.

Acknowledgements. The authors thank the financial support by Centre national d'études spatiales (CNES), and by the Italian Space Agency (grants ASI/INAF n. 2018-27-HH.0 and 2022-12-HH.0). IB thanks the French PAUSE program, which provides support to scientists at risk. This work utilized data obtained from the Asteroid Lightcurve Data Exchange Format (ALCDEF) database, which is supported by funding from NASA grant 80NSSC18K0851. The light curve observations obtained by E.F Mananes are appreciated.

References

Barucci, M. A., Dotto, E., Brucato, J. R., et al. 2002, Icarus, 156, 202
Barucci, M. A., Fornasier, S., Dotto, E., et al. 2008, A&A, 477, 665
Binzel, R. P., Rivkin, A. S., Stuart, J. S., et al. 2004, Icarus, 170, 259
Binzel, R. P., DeMeo, F. E., Turtelboom, E. V., et al. 2019, Icarus, 324, 41
Delbo, M. 2004, PhD Thesis, Free University of Berlin, Germany
Delbo, M., Walsh, K., Mueller, M., Harris, A. W., & Howell, E. S. 2011, Icarus, 212, 138
Delbo, M., Mueller, M., Emery, J. P., Rozitis, B., & Capria, M. T. 2015, in Asteroids IV, 107
DeMeo, F. E., Binzel, R. P., Slivan, S. M., & Bus, S. J. 2009, Icarus, 202, 160
Dotto, E., Müller, T. G., Barucci, M. A., et al. 2000, A&A, 358, 1133
Dotto, E., Barucci, M. A., Brucato, J. R., Müller, T. G., & Carvano, J. 2004, A&A, 427, 1081
Fatka, P., Pravec, P., Kusnirak, K., et al. 2023, in 8th IAA Planetary Defence Conference
Fornasier, S., Dotto, E., Marzari, F., et al. 2004, Icarus, 172, 221
Geem, J., Ishiguro, M., Granvik, M., et al. 2023, MNRAS, 525, L17
Harris, A. W. 1989, Lunar Planet. Sci. Conf., 20, 375
Harris, A. W. 1998, Icarus, 131, 291
Harris, A. W., & Drube, L. 2016, ApJ, 832, 127
Harris, A., & Warner, B. D. 2020, Icarus, 339, 113602a
Hirabayashi, M., Mimasu, Y., Sakatani, N., et al. 2021, Adv. Space Res., 68, 1533
Houck, J. R., Roellig, T. L., van Cleve, J., et al. 2004, ApJS, 154, 18
Lamy, P. L., Jorda, L., Fornasier, S., et al. 2008, A&A, 487, 1187
Landolt, A. U. 1992, AJ, 104, 340
Lazzarin, M., Marchi, S., Magrin, S., & Licandro, J. 2005, MNRAS, 359, 1575
Lebofsky, L. A., Sykes, M. V., Tedesco, E. F., et al. 1986, Icarus, 68, 239
Mainzer, A., Grav, T., Bauer, J., et al. 2011, ApJ, 743, 156
Mainzer, A., Grav, T., Masiero, J., et al. 2012, ApJ, 752, 110
Mainzer, A., Bauer, J., Grav, T., et al. 2014, ApJ, 784, 110
Muinonen, K., Belskaya, I. N., Cellino, A., et al. 2010, Icarus, 209, 542
Novaković, B., Fenucci, M., Marčeta, D., & Pavela, D. 2024, Planet. Sci. J., 5, 11
Pravec, P., Harris, A. W., Kušnirák, P., Galád, A., & Hornoch, K. 2012, Icarus, 221, 365
Salisbury, J. W., Daria, D. M., & Jarosewich, E. 1991a, in NASA, Washington, Reports of Planetary Geology and Geophysics Program, (SEE N92–10728 01–91), 262
Salisbury, J. W., D'Aria, D. M., & Jarosewich, E. 1991b, Icarus, 92, 280
Sunshine, J. M., Connolly, H. C., McCoy, T. J., Bus, S. J., & La Croix, L. M. 2008, Science, 320, 514
Warner, B. D. 2023, Minor Planet. Bull., 50, 217
Warner, B. D., Harris, A. W., & Pravec, P. 2009, Icarus, 202, 134
Werner, M. W., Roellig, T. L., Low, F. J., et al. 2004, ApJS, 154, 1
Wolters, S. D., Green, S. F., McBride, N., & Davies, J. K. 2008, Icarus, 193, 535
Wright, E., Masiero, J., & Mainzer, A. 2023, BAAS, 55, 107.03
Zappala, V., Cellino, A., Barucci, A. M., Fulchignoni, M., & Lupishko, D. F. 1990, A&A, 231, 548

Appendix A: Supplementary material: Tables and figures

Table A.1. Observing circumstances, magnitude, and colors of (98943) 2001 CC21 from the 3.5 m NTT, 1.2 m OHP, and 0.7 m Abastumani telescopes. * plus one day.

Telescope	date	UT	r (AU)	Δ (AU)	α (°)	V	R	B-V	V-R	V-I
3.5m NTT	31-10-2005	03:18–03:26	1.108	0.418	63.2	19.27±0.02			0.44±0.02	0.85±0.03
1.2m OHP	26-11-2022	01:36–02:30	1.253	0.496	47.4	19.83±0.03		0.95±0.06	0.39±0.05	
1.2m OHP	30-11-2022	03:25–04:31	1.250	0.469	46.4	19.71±0.03		0.85±0.04	0.47±0.03	0.82±0.09
0.7m Abas.	22-01-2023	18:08–02:44*	1.149	0.179	21.4		15.99±0.03			
0.7m Abas.	06-01-2024	15:05–20:25	1.226	0.268	22.4		17.17±0.05			
0.7m Abas.	15-01-2024	15:37–21:10	1.209	0.286	33.4		17.63±0.05			

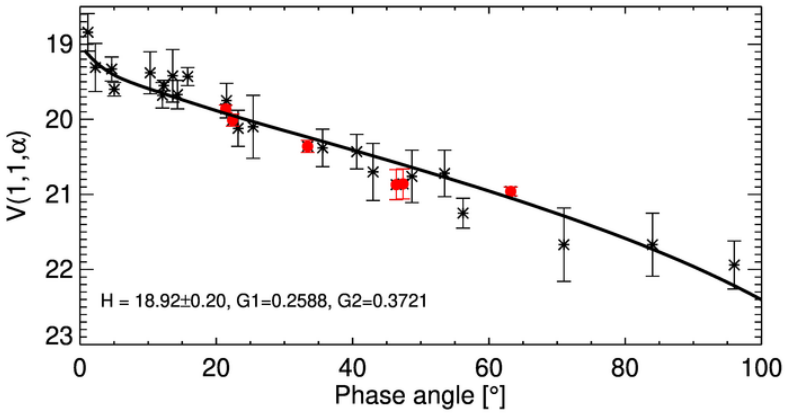

Fig. A.1. HG1G2 fit of the photometric data presented here (Table A.1, red circles), together with data from astrometry available from the MPC database.

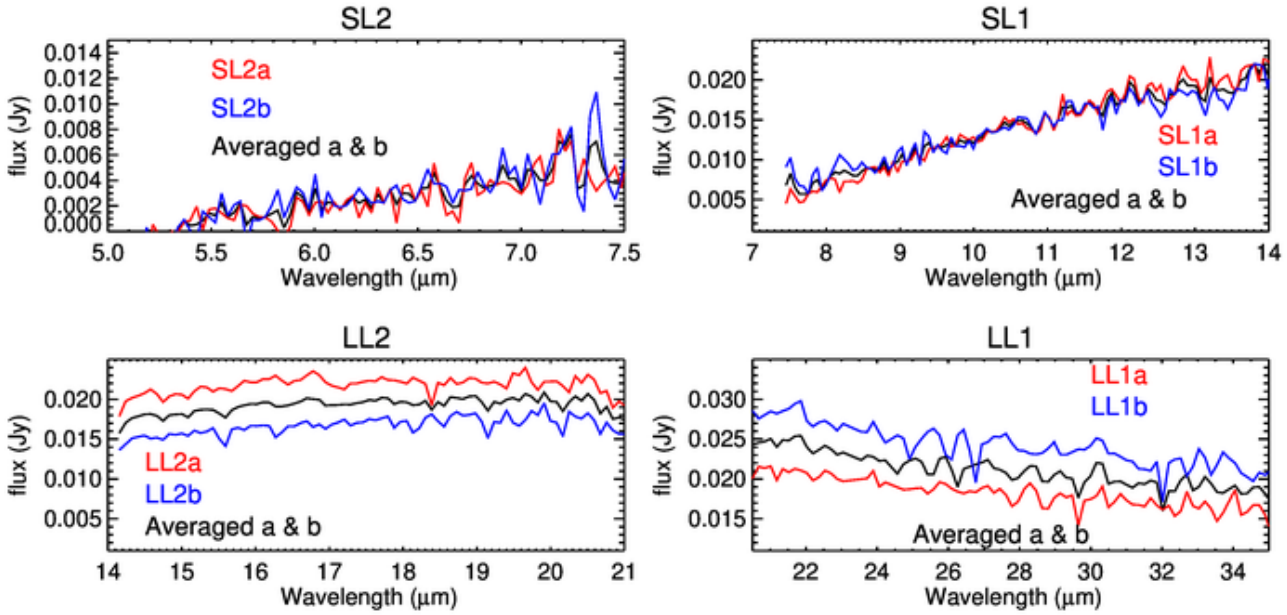

Fig. A.2. Spectral energy distribution of the individual a and b spectra in red and blue, respectively, for the four IRS segments. In black is the average spectrum for each segment.

Appendix B: Thermal model

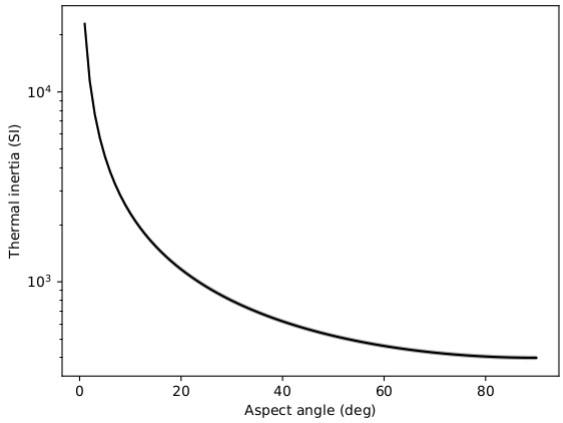

Fig. B.1. Variation in the thermal inertia (SI stands for international system units, which for thermal inertia are J m^{-2} $s^{-0.5}$ K^{-1}) as a function of the aspect angle, estimated from Eq. 2 of Harris & Drube (2016).

The NEATM model we use (Harris 1998) assumes that the asteroid surface temperature, $T(\theta)$, is controlled only by geometry, namely the subsolar latitude θ, on the asteroid surface. This temperature is a simple function of the subsolar temperature T_{SS}, i.e. $T(\theta) = T_{SS}(\cos\theta)^{\frac{1}{4}}$ for $\theta \leq 90^o$ and T(θ)=0 for $\theta > 90^o$, with $T_{SS} = \left(S_\odot(1-A)r^{-2}(\eta\epsilon\sigma)^{-1}\right)^{0.25}$, where A is the bolometric Bond albedo, r the heliocentric distance of the asteroid, $S_\odot$ is the solar constant at 1 au from the Sun, σ is the Stefan Boltzmann constant, ϵ is the emissivity, and η is the so-called beaming parameter. In NEATM, an initial guess is made for the geometric albedo p_V and η value, so that the diameter D and the A-value of the asteroid are calculated from $D(km) = 1329\ 10^{-H/5} \times (p_V)^{-0.5}$ and $A = q\ p_V$, where H is the absolute magnitude, and q the phase integral (Harris 1998). Once the temperature distribution is calculated as described above, the infrared flux $f(\lambda)$ is derived from the Planck function multiplied by the emissivity, integrated over the visible heated portion of the model asteroid shape – which is controlled only by the phase angle (Harris 1998) – and multiplied by the factor D^2/Δ^2, where Δ is the asteroid-observer distance in au. The model flux is compared to the observed one by calculating a χ^2 figure of merit. A least-square fit is performed by minimizing the χ^2 as a function of the model parameters D, η, and p_V (or A), to obtain a NEATM solution and its accuracy in terms of size, beaming parameter, and albedo.